NUCL SCI TECH (2020) 31:10
https://doi.org/10.1007/s41365-019-0720-1

Transmutation of ^{129}I in a single-fluid double-zone thorium molten salt reactor

Kun-Feng Ma[1,2,3] · Cheng-Gang Yu[1,2] · Xiang-Zhou Cai[1,2,3] · Chun-Yan Zou[1,2] · Jin-Gen Chen[1,2,3]

Received: 29 September 2019 / Revised: 11 November 2019 / Accepted: 12 November 2019 / Published online: 3 January 2020

Abstract Herein, we assess the ^{129}I transmutation capability of a 2250-MWt single-fluid double-zone thorium molten salt reactor (SD-TMSR) by considering two methods. One is realized by loading an appropriate amount of ^{129}I before the startup of the reactor, and the amount of ^{129}I during operation is kept constant by online feeding ^{129}I. The other adopts only an initial loading of ^{129}I before startup, and no other ^{129}I is fed online during operation. The investigation first focuses on the effect of the loading of I on the Th-^{233}U isobreeding performance. The results indicate that a ^{233}U isobreeding mode can be achieved for both scenarios for a 60-year operation when the initial molar proportion of LiI is maintained within 0.40% and 0.87%, respectively. Then, the transmutation performances for the two scenarios are compared by changing the amount of injected iodine into the core. It is found that the scenario that adopts an initial loading of ^{129}I shows a slightly better transmutation performance in comparison with the scenario that adopts online feeding of ^{129}I when the net ^{233}U productions for the two scenarios are kept equal. The initial loading of ^{129}I scenario with LiI = 0.87% molar proportion is recommended for ^{129}I transmutation in the SD-TMSR, and can transmute 1.88 t of ^{129}I in the ^{233}U isobreeding mode over 60 years.

Keywords ^{129}I transmutation · Thorium molten salt reactor · Th-U isobreeding

1 Introduction

Long-lived (over 10^5 years) fission products (LLFPs) are the primary contributors to the radioactive hazards of nuclear waste, which impede the sustainable development of nuclear energy. Because of its long half-life of 1.60×10^7 years, large radiotoxicity coefficient of 2.70×10^{-1} Sv/g, and high geochemical mobility [1], ^{129}I is one of the most important LLFPs. The annual production amount of ^{129}I is about 5 kg in a traditional 1000-MWe pressurized water reactor (PWR), which accounts for a mass fraction of about 80% in the iodine isotopes. The other 20% is provided by the stable isotope of ^{127}I [2].

Transmutation is an effective way to eliminate or minimize the radioactive hazard of ^{129}I [3]. When ^{129}I captures a neutron, it emits an electron and becomes stable ^{130}Xe. For the transmutation of ^{129}I, ^{127}I in the iodine isotopes must also be considered since the isotope separation of ^{129}I is very complex and costly. Thus, some ^{129}I will be produced from ^{127}I by two sequential neutron captures. Fortunately, both ^{127}I and its daughter product of ^{128}I have relatively small thermal neutron capture cross sections of 6.1 b and 3.7 b, respectively. In addition, ^{128}I with a half-

This work was supported by the Chinese TMSR Strategic Pioneer Science and Technology Project (No. XDA02010000) and the Frontier Science Key Program of the Chinese Academy of Sciences (No. QYZDY-SSW-JSC016).

✉ Chun-Yan Zou
zouchunyan@sinap.ac.cn

✉ Jin-Gen Chen
chenjg@sinap.ac.cn

1 Shanghai Institute of Applied Physics, Chinese Academy of Sciences, Shanghai 201800, China

2 CAS Innovative Academies in TMSR Energy System, Chinese Academy of Sciences, Shanghai 201800, China

3 University of Chinese Academy of Sciences, Beijing 100049, China

life of 0.4 h will quickly decay to stable ^{128}Xe, which is also beneficial in reducing the production of ^{129}I from ^{127}I.

The transmutation of ^{129}I has been extensively investigated in different types of reactors including the accelerator driven system (ADS) [4, 5], fast reactor [6, 7], and PWR [8, 9]. For the ^{129}I transmutation in ADS, Song et al. [4] performed a systematic study by loading double-annular LLFP target assemblies with CaI_2 in the reflector region of an ADS. Afterward, Ismailov et al. [5] improved the ^{129}I transmutation rate by loading the sodium iodide assembly in both the core and the surrounding core region, and a transmutation rate of ^{129}I up to 46 kg/y was achieved in an 800-MWt ADS. Regarding the ^{129}I transmutation in a fast reactor, Wakabayshi [7] investigated the ^{129}I transmutation performance by loading NaI in the blanket region of a 1600-MWt fast reactor, and about 18 kg/y of ^{129}I was transmuted. The ^{129}I transmutation in a thermal reactor is also recognized as a promising method owing to the large thermal neutron capture cross section of ^{129}I and the mature operation technology of PWR. Recently, Liu et al. [9] studied the ^{129}I transmutation capability in a 1000-MWe PWR by loading the MgI_2 target in the guide tube and discrete pins. The discrete pin loading scenario provided an excellent ^{129}I transmutation capability of 20.25 kg/y.

Recently, a liquid-fueled reactor concept of a molten salt reactor (MSR) was investigated for the ^{129}I transmutation [10]. MSR has many fascinating characteristics including inherent safety, excellent neutron economy, no fuel fabrication, online refueling, and reprocessing [11]. Different from the ^{129}I transmutation in a solid-fuel reactor where only a small portion of ^{129}I can be loaded in the irradiation targets, MSR allows for a large amount of iodine to be initially loaded and/or continuously added to the fuel salt during the reactor operation, implying an attractive potential of ^{129}I transmutation in an MSR. The ^{129}I transmutation capacity for a 2500-MWt thorium molten salt reactor (TMSR) was evaluated. The inventory of ^{129}I was kept constant (290 kg) by online feeding ^{129}I into the fuel salt during the reactor operation based on the ^{233}U isobreeding mode. The transmutation capacity of ^{129}I in the TMSR was 10.2 kg/y [10]. Nevertheless, the ^{129}I transmutation weakened the Th-U breeding or conversion capacity of the reactor because a considerable number of neutrons in the core can be absorbed by ^{129}I instead of ^{232}Th. This means that an MSR with a higher Th-U breeding/conversion capacity may offer a remarkably higher ^{129}I transmutation capability.

A single-fluid double-zone thorium molten salt reactor (SD-TMSR) was proposed by optimizing the ratios of molten salt and graphite in both the inner and the outer fuel assemblies [12]. The Th-U breeding ratio of SD-TMSR was about 1.08, which is significantly larger than that of the above TMSR. Hence, we focus on evaluating the ^{129}I transmutation based on the SD-TMSR under the ^{233}U isobreeding condition. The initial and online loadings of ^{129}I are analyzed to compare their ^{129}I transmutation performances as well as their influences on reactor operation. Section 2 describes the SD-TMSR and the calculation tool. Results and discussions are presented in Sect. 3. Section 4 gives the conclusions.

2 Description of SD-TMSR and calculation tool

2.1 Core description

The SD-TMSR is a 2250-MWt reactor with a thermal neutron spectrum. Figure 1 shows a quarter vertical geometry model of the SD-TMSR including the fuel salt, graphite moderator and reflectors, B_4C neutron protection layer, and Hastelloy N alloy vessel. The main parameters of the SD-TMSR are listed in Table 1. The total fuel salt volume is 52.9 m^3, which is distributed in the inner and outer zones in the core, top plenum, bottom plenum, and heat exchanger. Fuel salt with a composition of 70 LiF–17.5 BeF_2–12.5 HNF_4 (mol%) is adopted in the SD-TMSR, where the ^{7}Li enrichment and the fuel salt density are 99.995% and 3.33 g/cm^3, respectively. The B_4C layer and Hastelloy N alloy vessel have an identical thickness of 10 cm.

2.2 Calculation tool

The MSR reprocessing sequence (MSR-RS) [13–15] is adopted in this work to simulate the iodine transmutation, which is coupled with the criticality analysis module (CSAS6), problem-dependent cross-section processing module (TRITON), and depletion and decay calculation module (ORIGEN-S) in the SCALE6.1 program. A

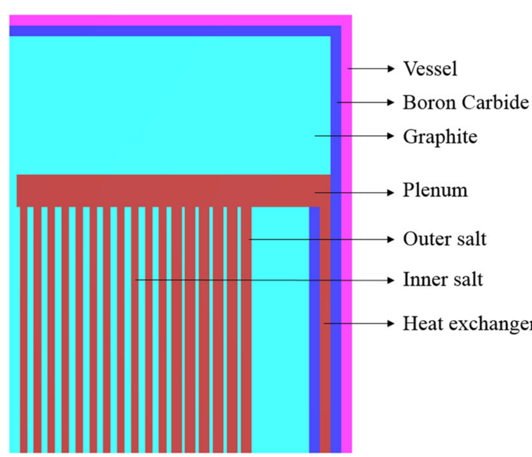

Fig. 1 Cross section of SD-TMSR

Table 1 Geometry parameters for core

Parameters	Value
Thermal power (MWt)	2250
Fuel volume (m^3)	52.9
Core diameter and height (cm)	460/460
Inscribed radius of graphite hexagonal prism (cm)	6.495
Inner fuel salt channel radius (cm)	3.5
Outer fuel salt channel radius (cm)	5
Thickness above and below salt plena (cm)	30
Thickness above, below, and side graphite (cm)	130/130/50
Thickness of B_4C (cm)	10
Fuel salt composition (mol%)	70 LiF–17.5 BeF_2–12.5 HNF_4
Fuel salt temperature (K)	900
Density of fuel salt at 900 K (g/cm^3)	3.3
Dilatation coefficient of fuel salt ($g/cm^3/K$)	-6.7×10^{-4}
Enrichment of ^7Li (mol%)	99.995
Density of graphite (g/cm^3)	2.3
Density of B_4C (g/cm^3)	2.52
Enrichment of ^{10}B (mol%)	18.4

flowchart of the MSR-RS is displayed in Fig. 2. First, the core geometry and molten salt compositions are initialized. Then, a criticality calculation is performed by CSAS6 based on the entire core, and a 238-group ENDF/B-VII cross-section database is used. A one-group cross-section library is generated by the TRITON calculation, which performs problem-dependent cross-section processing followed by a multigroup neutron transport calculation. The burnup calculation is performed by ORIGEN-S with online reprocessing and refueling. During each burnup time step, the molten salt compositions are modified following a reprocessing scheme set by the user and are followed by another CSAS6 calculation step to obtain a new neutron flux and a new k_{eff} determined by both depletion and refueling. Then, a new TRITON input file is produced for the next-step burnup calculation. The cycle calculation is performed iteratively until the cycle time reaches the value set by the user. The MSR-RS was verified in our previous work [12–16].

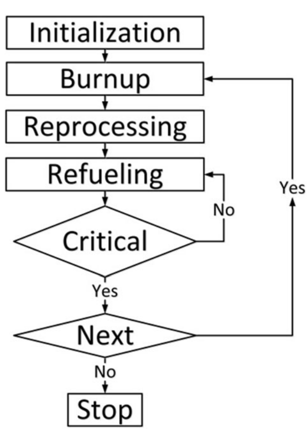

Fig. 2 Flowchart of MSR-RS

In this MSR-RS, the gaseous and noble metallic FPs in the fuel salts are removed online through a helium bubbling system with a constant separation time of 30 s and separation efficiency of 100%. The other soluble FPs are continuously removed, and Pa is extracted online by chemical reprocessing at a reprocessing rate of 5 m^3/d and separation efficiency of 100% [12]. In addition, ^{232}Th and ^{233}U are injected online into the fuel salt to maintain the reactor criticality and the total actinide inventory constant for the stability of the molten salt.

3 Results and discussion

The online feeding and initial loading of ^{129}I scenarios are introduced in this section. Then, the net ^{233}U production of the SD-TMSR for the above scenarios is analyzed by varying the LiI loading to obtain a Th-^{233}U isobreeding. Finally, the ^{129}I transmutation performances for the above scenarios with different LiI loadings are compared.

3.1 I transmutation scenarios

It is essential to select a proper chemical compound of iodine to minimize its effects on the fuel salt component of SD-TMSR. Several iodide forms such as ThI_4, UI_4, BeI_2, and LiI have been investigated during the past several decades. Compared with ThI_4, UI_4, and BeI_2, LiI is more appropriate for ^{129}I transmutation because it has excellent stability in air and can be dissolved into the molten salt at a large amount [17]. Hence, LiI is chosen as sample form and is loaded into the fuel salt to substitute for some LiF in the FLiBe carrier salt. For instance, the fuel salt composition becomes 69 LiF–1 LiI–17.5 BeF_2–12.5 HNF_4 (mol%) if 1.0 mol% of LiI is loaded into the fuel salt.

An analysis of the ^{129}I transmutation scenario (named scenario 1) is performed by online feeding ^{129}I into the fuel salt to keep the ^{129}I amount in the core constant during the SD-TMSR operation. Nevertheless, the online feeding of ^{129}I is relatively complex for the SD-TMSR operation because it requires an accurate monitoring of the ^{129}I inventory both in the core and online feed during the entire operation. Considering the disadvantages in scenario 1, we propose an alternative ^{129}I transmutation (scenario 2) in which ^{129}I is initially loaded into fuel salt before the startup of the reactor, and no other ^{129}I is fed into the fuel salt during the reactor operation. A large loading of ^{129}I may improve the transmutation capacity of ^{129}I. However, the physicochemical properties of the fuel salt may be changed when a large amount of LiI is loaded. In addition, more ^{233}U is loaded into the fuel salt to maintain the reactor criticality, which is disadvantageous from the standpoint of Th-U fuel breeding. Hence, a proportion of 1% LiI is adopted as the upper limit to minimize the change in the fuel salt component.

3.2 Th-^{233}U isobreeding performance

Owing to the larger thermal neutron absorption cross section of ^{129}I compared with ^{19}F, more thermal neutrons in the core are absorbed when ^{19}F is replaced by ^{129}I in the fuel salt, which hardens the neutron spectrum of the SD-TMSR (see Fig. 3). Therefore, more ^{233}U loading is required to maintain the reactor criticality when a large amount of iodine is loaded into the fuel salt. Figure 4 shows the initial ^{129}I inventory and the required initial ^{233}U loading as a function of the LiI molar proportion under the critical condition ($k_{eff} \approx 1$). When the LiI proportion increases from 0 to 1.0 mol%, the increment of initial ^{129}I loading is about 2.7 t, and the corresponding ^{233}U mass increases almost linearly by about 0.35 t.

The burnups for the above two ^{129}I transmutation scenarios with different LiI loading proportions are simulated by the MSR-RS for up to 60 years. The Th-U breeding performance can be evaluated by the net ^{233}U production, which is defined as [18, 19]

$$^{233}\mathrm{U}\,(\mathrm{production}) = {}^{233}\,\mathrm{U}\,(\mathrm{residue}) + {}^{233}\,\mathrm{Pa}\,(\mathrm{extract}) - {}^{233}\,\mathrm{U}\,(\mathrm{inject}), \quad (1)$$

where ^{233}U (inject) is the total injected ^{233}U amount into the core, which includes the initially loaded and online-fed ^{233}U masses; ^{233}Pa (extract) is the extracted mass of ^{233}Pa from the core; and ^{233}U (residue) is the residual mass of ^{233}U in the core. A positive value of the net ^{233}U production means that more ^{233}U can be bred than consumed in the core, while a negative value indicates that the produced ^{233}U in the core is insufficient to compensate for the consumed ^{233}U, and additional ^{233}U from other reactors should be fed into the core to maintain the reactor criticality.

The evolutions of the net ^{233}U production and inventories of key nuclides for both scenarios with LiI = 1.0% are presented in Fig. 5. For scenario 1, the net ^{233}U production monotonically decreases during the 60 years of operation, while the ^{233}U inventory in the core increases gradually with the operation time. In particular, some actinides generated from ^{233}U, including nonfissile isotopes (e.g., ^{234}U) and fissile isotopes (e.g., ^{235}U), also keep accumulating in the reactor. The generation of new fissile isotopes is insufficient to compensate for the negative reactivity

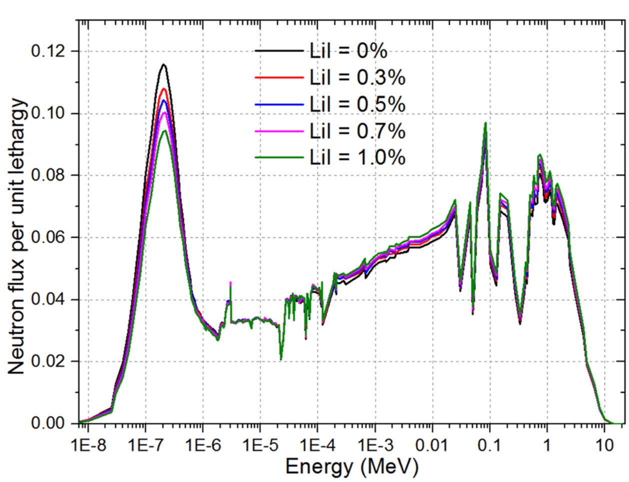

Fig. 3 (Color online) Comparison of initial neutron spectra for different ^{129}I loadings

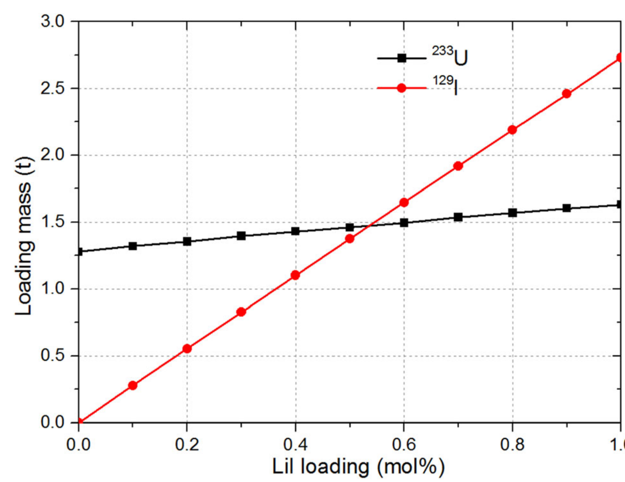

Fig. 4 Initial ^{233}U and ^{129}I loadings as a function of ^{129}I molar proportion under critical condition

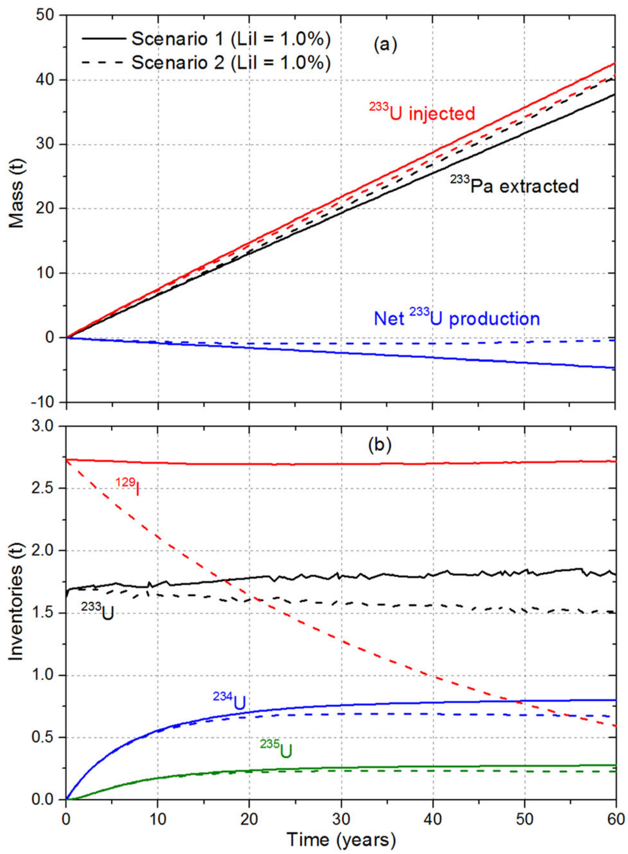

Fig. 5 (Color online) **a** Net ^{233}U production and **b** inventory of nuclides for both scenarios (LiI = 1.0%) during 60 years of operation

inserted by the accumulation of new nonfissile isotopes during the operation. Hence, additional ^{233}U has to be injected into the core to maintain the reactor criticality, which makes the ^{233}U amount in the core increase gradually from 1.63 t at startup to 1.81 t at the end of life, as shown in Fig. 5b. During the first two years, the slight increase in ^{233}U amount in the core is primarily caused by the accumulated FPs since no considerably heavier actinides are produced in the core for such a short operation time. To maintain the critical operation of the SD-TMSR for 60 years, the total fed mass of ^{233}U is about 42.69 t. Meanwhile, the total extracted mass of ^{233}Pa is about 37.89 t, which is 4.80 t smaller than the total fed mass of ^{233}U. Hence, according to Eq. (1), the net ^{233}U production for scenario 1 is about − 4.62 t at the end of life (LiI = 1.0%).

By contrast, the ^{129}I inventory in the core for scenario 2 decreases from 2.73 t at startup to 0.59 t at the end of life since no ^{129}I is fed online into the core during operation. The decrease in ^{129}I inventory in the core induces a positive reactivity that exceeds the total negative reactivity caused by the neutron absorption of accumulated FPs and heavier actinides during the entire operation. Therefore, the ^{233}U inventory in the core decreases from 1.63 t at startup to 1.53 t at the end of life. However, the initially loaded ^{233}U is insufficient to maintain the critical operation of the core in the depletion process owing to its fission depletion and the accumulation of FPs and heavier actinides. Therefore, ^{233}U should be continuously fed into the fuel salt to maintain the reactor criticality during the entire operation. For the 60-year operation, k_{eff} of the core is kept at ∼ 1.0 by the online feeding of ^{233}U and Th. In addition, with a lower total ^{129}I inventory in the core, the transmutation rate of ^{129}I for scenario 2 in the depletion process is much smaller than that for scenario 1, which indicates that scenario 2 requires less ^{233}U to compensate for the negative reactivity by ^{129}I than scenario 1. In other words, ^{233}U is refueled online into the core to primarily compensate for its fission consumption for scenario 2, which leads to a much smaller amount of externally fed ^{233}U fuel than scenario 1. The net ^{233}U production for scenario 2 is − 0.43 t at the end of life, which is 4.19 t greater than that for scenario 1, as shown in Fig. 5a.

One can also find from Fig. 5 that the net ^{233}U production for both scenarios has significantly different evolution trends and always changes with the operation time. Considering the negative net ^{233}U production for both scenarios (LiI = 1.0%) at the end of life, the dependence of net ^{233}U production on varying LiI loading is presented in Fig. 6. The loss rate of the net ^{233}U production for scenario 2 is much smaller than that for scenario 1 because the total ^{129}I loading amount of the core for the former is much smaller than that for the latter. For instance, the total ^{129}I loading amount of the core for scenario 2 (LiI = 1.0%) is 2.73 t, which is 3.67 t smaller than that for scenario 1 (LiI = 1.0%) because no ^{129}I is fed online into the core for scenario 2 (LiI = 1.0%). It is found that when the initial molar proportions of LiI for both scenarios are maintained within ∼ 0.40% and 0.87%, respectively, the net ^{233}U

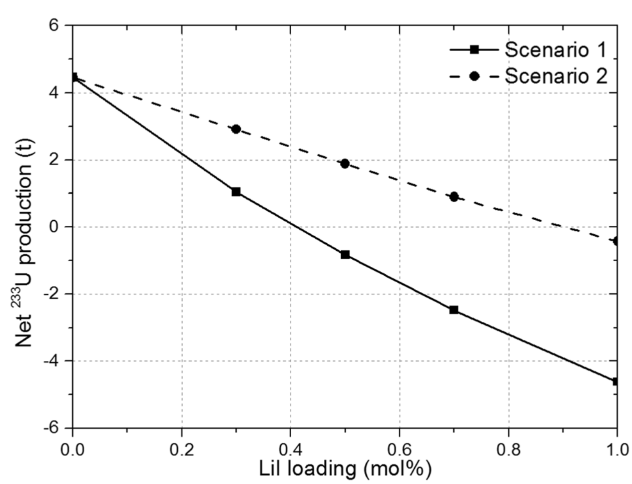

Fig. 6 (Color online) Net ^{233}U production at end of life as a function of initial loading of LiI for scenarios 1 and 2

production is equal to 0 t, indicating that a ^{233}U isobreeding mode for both scenarios can be achieved for a 60-year operation in the SD-TMSR, as shown in Fig. 6.

3.3 Transmutation capability of ^{129}I

The ^{129}I transmutation capability of the SD-TMSR can be evaluated by two important parameters: transmuted mass and fraction. The transmuted fraction is defined as

$$\mathrm{TF}(t) = \frac{\Delta M(t)}{M_0(t)}, \tag{2}$$

where $M_0(t)$ is the injected mass of ^{129}I into the core, which includes the initially loaded and online-fed ^{129}I masses at operating time t. $\Delta M(t)$ is the transmuted mass of ^{129}I, which is equal to the difference between the injected mass and the residual mass of ^{129}I in the core at operating time t.

Figure 7 presents the evolutions of the transmuted mass, injected mass, and transmuted fraction of ^{129}I for both scenarios (LiI = 1.0%). It is found that the transmuted mass of ^{129}I for scenario 2 increases with the operation time, but the transmutation rate decreases with the operation time compared to scenario 1 because of the decrease in ^{129}I inventory in the core (see Fig. 5b). Therefore, the transmuted mass of ^{129}I for scenario 2 is about 2.14 t at the end of life, which is 1.53 t smaller than that for scenario 1. However, the transmuted fraction of ^{129}I for the former is 78.34% at the end of life, which is 20.83% greater than that for the latter.

To investigate the relationship between the transmutation capability of ^{129}I and net ^{233}U production, the transmuted mass and fraction of ^{129}I at the end of life as a function of the net ^{233}U production for both scenarios are presented in Fig. 8. The transmuted mass of ^{129}I for scenario 2 is slightly larger than that for scenario 1 under an identical net ^{233}U production condition, indicating that scenario 2 is superior to scenario 1. When the SD-TMSR achieves a ^{233}U isobreeding mode, the transmuted mass of ^{129}I for scenario 2 is about 1.88 t, which is 0.16 t greater than that for scenario 1. In addition, the transmuted fraction for the former is 78.96%, which is also significantly larger than that for the latter (65.50%). The transmuted mass and fraction of ^{129}I and the net ^{233}U production for both scenarios with different LiI loadings are listed in Tables 2 and 3, respectively.

In order to investigate the difference in ^{129}I transmutation performance under the ^{233}U isobreeding mode between the above two scenarios, the evolutions of the transmuted mass and inventory of ^{129}I are displayed in Fig. 9. For scenario 1, the transmuted mass of ^{129}I increases linearly with the operation time, which is about 1.72 t at the end of life owing to the constant inventory of ^{129}I in the core. This indicates that the transmutation rate of ^{129}I can stay almost constant at about 28.67 kg/y. By contrast, the transmuted mass of ^{129}I for scenario 2 is about 1.88 t at the end of life, while the transmutation rate declines with the operation time owing to the decrease in ^{129}I inventory in the core. Hence, the transmuted mass of ^{129}I for scenario 2 is larger than that for scenario 1 during the 60 years of operation. However, most of the ^{129}I for scenario 2 is transmuted during the first 30 years and is about 1.28 t, which is much greater than that during the remaining 30 years at 0.6 t. Considering its higher transmutation performance and simpler operation of the reactor, scenario 2 with an initial molar proportion of LiI = 0.87% is recommended for the ^{129}I transmutation in the SD-TMSR.

The transmutation capability of ^{129}I in the SD-TMSR is also compared with other reactors in Table 4. The supportive factor is defined as the ratio of the transmuted mass of ^{129}I in the different reactors to the yield of ^{129}I in a

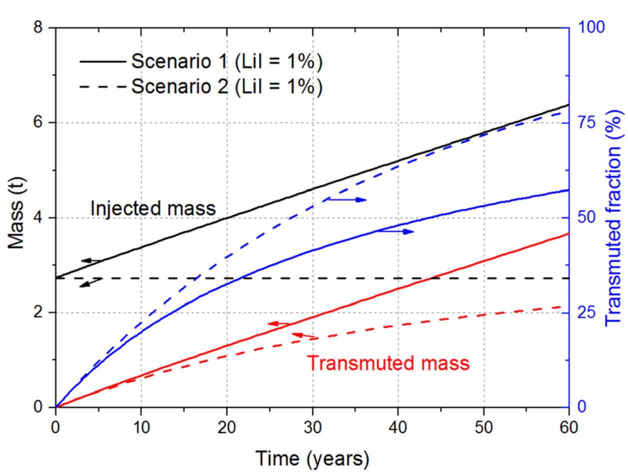

Fig. 7 (Color online) Transmuted mass, injected mass, and transmuted fraction of ^{129}I for scenarios 1 and 2 (LiI = 1.0%) during 60 years of operation

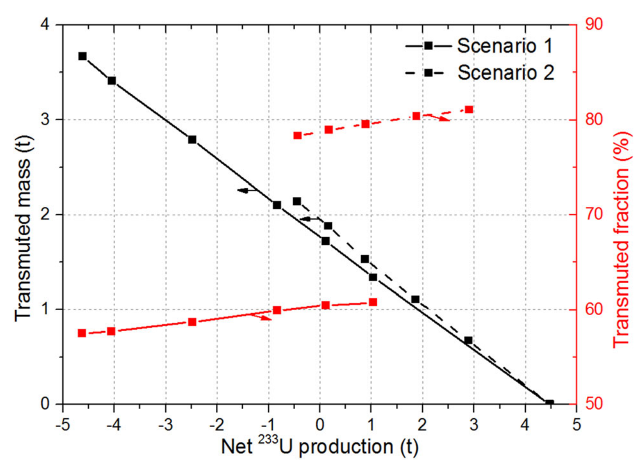

Fig. 8 (Color online) Transmuted mass and fraction of ^{129}I as a function of net ^{233}U production for scenarios 1 and 2 at end of life

Table 2 Transmutation performances for scenario 1 at end of life

Initial molar proportion (%)	0	0.30	0.40	0.50	0.70	0.90	1.00
Initially loaded ^{129}I (t)	0	0.83	1.10	1.38	1.92	2.46	2.73
Fed ^{129}I (t)	0	1.37	1.74	2.13	2.81	3.45	3.67
Residual ^{129}I at the end of life (kg)	1.86	862.48	1124.96	1404.61	1943.66	2498.98	2718.29
Transmuted mass of ^{129}I (kg)	− 1.86	1337.30	1722.66	2102.56	2778.36	3412.77	3668.97
Transmuted fraction of ^{129}I (%)	–	60.79	60.50	59.95	58.73	57.73	57.51
Net ^{233}U production (t)	4.46	1.04	0.12	− 0.83	− 2.48	− 4.05	− 4.62

Table 3 Transmutation performances for scenario 2 at end of life

Initial molar proportion (%)	0	0.30	0.50	0.70	0.87	0.90	1.00
Initially loaded ^{129}I (t)	0	0.83	1.38	1.92	2.38	2.46	2.73
Residual ^{129}I at the end of life (kg)	1.86	156.61	270.28	392.42	500.61	521.05	589.82
Transmuted mass of ^{129}I (kg)	− 1.86	671.62	1105.48	1527.21	1878.47	1938.83	2138.84
Transmuted fraction of ^{129}I (%)	–	81.09	80.35	79.56	78.96	78.82	78.34
Net ^{233}U production (t)	4.46	2.91	1.88	0.89	0.18	− 0.01	− 0.43

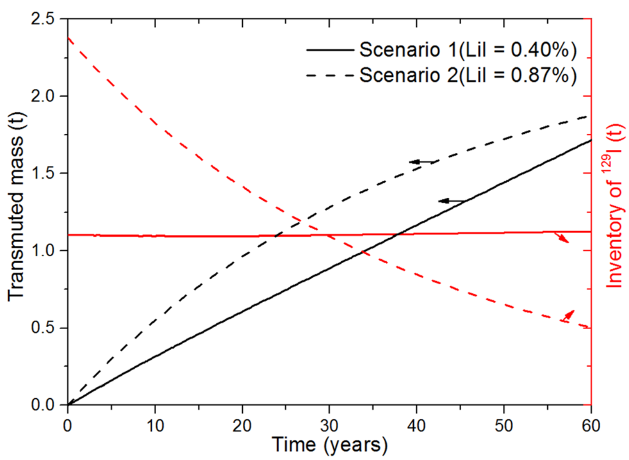

Fig. 9 (Color online) Transmuted and residual mass of ^{129}I for scenario 1 (LiI = 0.40%) and scenario 2 (LiI = 0.87%) during 60 years of operation

traditional 1000-MWe PWR under normalized thermal output and operation time [20]. The transmutation rate, supportive factor, and transmuted fraction of the SD-TMSR are 13.92 g/(MWt y), 8.19, and 78.96%, respectively, which are significantly larger than those of the TMSR. The SD-TMSR also exhibits an excellent ^{129}I transmutation performance compared with the PWR and the fast reactor. Although the transmutation rate and supportive factor of the SD-TMSR are much smaller than those of the ADS, the transmuted fraction of the former is significantly larger than that of the latter since the solid ^{129}I target in a solid-fuel reactor cannot undergo long-term operation owing to its mechanism and irradiation performance.

4 Conclusion

A systematic study of the ^{129}I transmutation in the SD-TMSR was performed. First, the initial ^{233}U loading as a function of ^{129}I loading was analyzed. Then, both the online feeding (scenario 1) and initial loading (scenario 2) of ^{129}I were analyzed to compare their transmutations and Th-U breeding capabilities. Conclusions drawn from the above analyses are as follows:

Table 4 Comparison of transmutation performances in different reactors

Type	Fast reactor	ADS	PWR	TMSR	SD-TMSR
Power (MWt)	1600	800	2941	2500	2250
Transmutation rate (g/MWt y)	11.25	57.50	6.88	4.08	13.92
Supportive factor	6.62	33.82	4.05	2.40	8.19
Transmuted fraction (%)	5.20	5.58	7.00	67.48	78.96

The initial ^{233}U loading was first analyzed for different LiI loadings from 0 to 1.0 mol%. When the initial loading proportion of LiI increased from 0 to 1%, the initial ^{233}U loading mass increased by 0.35 t to maintain the reactor criticality since the neutron spectrum of the core became harder. Then, the Th-U breeding performance and ^{129}I transmutation capability for both scenarios were investigated with different LiI molar proportions in the fuel salt. A large loading of ^{129}I is a disadvantage to the Th-U breeding or conversion of the reactor. When the loading proportion of LiI increased from 0 to 1 mol%, the net ^{233}U production for scenario 1 at the end of life decreased from 4.46 to − 4.62 t, while that for scenario 2 at the end of life decreased from 4.46 to − 0.43 t. To achieve ^{233}U isobreeding for the two scenarios, the initial molar proportion of LiI had to be kept within 0.40% for scenario 1 and 0.87% for scenario 2. Under the ^{233}U isobreeding mode, the transmuted mass and fraction of ^{129}I for scenario 2 were about 1.88 t and 78.96%, respectively, which are larger than those for scenario 1. Accordingly, an initial loading of ^{129}I scenario with LiI = 0.87% is recommended for the ^{129}I transmutation in the SD-TMSR. The transmutation rate, supportive factor, and transmuted fraction of SD-TMSR were 14.36 g/(MWt y), 8.45, and 78.96%, respectively, which are significantly larger than those of the PWR and fast reactor. In addition, the transmuted fraction of ^{129}I in the SD-TMSR was also significantly larger than that of ADS owing to its continuous transmutation.

References

1. W.S. Yang, Y. Kim, R.N. Hill et al., Long-lived fission product transmutation studies. Nucl. Sci. Eng. **146**, 291–318 (2004). https://doi.org/10.13182/NSE04-A2411
2. L.H. Baetslé, M. Embid-Segura, J. Magill et al., Implications of partitioning and transmutation in radioactive waste management, in *IAEA-TECDOC-435*, vol. 51 (IAEA, Vienna, Austria, 2004)
3. T.X. Liang, C.H. Tang, Transmutation of long-lived nuclides. Nucl. Tech. **26**(12), 935–939 (2003). https://doi.org/10.3321/j.issn:0253-3219.2003.12.008 **(in Chinese)**
4. T.Y. Song, Y. Kim, B.O. Lee et al., Design and analysis of HYPER. Ann. Nucl. Energy **34**, 902–909 (2007). https://doi.org/10.1016/j.anucene.2007.04.010
5. K. Ismailov, K. Nishihara, M. Saito et al., Optimization study on accelerator driven system design for effective transmutation of Iodine-129. Ann. Nucl. Energy **56**, 136–142 (2013). https://doi.org/10.1016/j.anucene.2013.01.042
6. T. Wakabayashi, N. Higano, Study on MA and FP transmutation in fast reactors. Prog. Nucl. Energy **32**, 555–562 (1998). https://doi.org/10.1016/S0149-1970(97)00043-7
7. T. Wakabayashi, Transmutation characteristics of MA and LLFP in a fast reactor. Prog. Nucl. Energy **40**, 457–463 (2002). https://doi.org/10.1016/S0149-1970(02)00038-0
8. K. Liu, H.C. Wu, L.Z. Cao et al., A code development for LLFP transmutation analysis based on the whole pin-wise calculation in PWRs. Nucl. Eng. Des. **256**, 56–66 (2013). https://doi.org/10.1016/j.nucengdes.2012.11.014
9. K. Liu, H.C. Wu, L.Z. Cao et al., Studies on LLFP transmutation in a pressurized water reactor. J. Nucl. Sci. Technol. **50**, 581–598 (2013). https://doi.org/10.1080/00223131.2013.785278
10. A. Nuttin, D. Heuer, A. Billebaud et al., Potential of thorium molten salt reactors: detailed calculations and concept evolution with a view to large scale energy production. Prog. Nucl. Energy **46**, 77–99 (2005). https://doi.org/10.1016/j.pnucene.2004.11.001
11. U.S. Doe, A technology roadmap for generation IV nuclear energy systems. Philos. Rev. **66**, 239–241 (2002)
12. G.C. Li, P. Cong, C.G. Yu et al., Optimization of Th-U fuel breeding based on a single-fluid double-zone thorium molten salt reactor. Prog. Nucl. Energy **108**, 144–151 (2018). https://doi.org/10.1016/j.pnucene.2018.04.017
13. C.G. Yu, X.X. Li, X.Z. Cai et al., Analysis of minor actinides transmutation for a molten salt fast reactor. Ann. Nucl. Energy **85**, 597–604 (2015). https://doi.org/10.1016/j.anucene.2015.06.014
14. D.Y. Cui, S.P. Xia, C.G. Yu et al., Methodologies for single-fluid, two-zone MSR burnup calculation based on SCALE/TRITON. Nucl. Tech. **40**(8), 080602 (2017). https://doi.org/10.11889/j.0253-3219.2017.hjs.40.080602 **(in Chinese)**
15. G.C. Li, Y. Zou, C.G. Yu et al., Influences of ^{7}Li enrichment on Th-U fuel breeding for an improved molten salt fast reactor (IMSFR). Nucl. Sci. Tech. **28**, 97 (2017). https://doi.org/10.1007/s41365-017-0250-7
16. C.G. Yu, C.Y. Zou, J.H. Wu et al., Development and verification of molten salt reactor refueling and reprocessing system analysis code based on SCALE. At. Energy Sci. Technol. **52**, 2126–2146 (2018). https://doi.org/10.7538/yzk.2018.youxian.0123 **(in Chinese)**
17. E. Capelli, O. Beneš, R.J.M. Konings, Thermodynamics of soluble fission products cesium and iodine in the molten salt reactor. J. Nucl. Mater. **501**, 238–252 (2018). https://doi.org/10.1016/j.jnucmat.2018.01.024
18. C.G. Yu, X.X. Li, X.Z. Cai et al., Minor actinide incineration and Th-U breeding in a small FLiNaK molten salt fast reactor. Ann. Nucl. Energy **99**, 335–344 (2017). https://doi.org/10.1016/j.anucene.2016.09.025
19. X.C. Zhao, D.Y. Cui, X.Z. Cai et al., Analysis of Th-U breeding capability for an accelerator-driven subcritical molten salt reactor. Nucl. Sci. Tech. **29**, 121 (2018). https://doi.org/10.1007/s41365-018-0448-3
20. H.L. Lu, Y. Ishiwatari, Y. Oka, Study on the LLFPs transmutation in a super-critical water-cooled fast reactor. Nucl. Eng. Des. **241**, 395–401 (2011). https://doi.org/10.1016/j.nucengdes.2010.10.019